

AperTO - Archivio Istituzionale Open Access dell'Università di Torino

Autoluminescent Metal-Organic Frameworks (MOFs): Self-Photoemission of a Highly Stable Thorium MOF

This is the author's manuscript

Original Citation:

Availability:

This version is available <http://hdl.handle.net/2318/1689763> since 2019-02-04T16:33:03Z

Published version:

DOI:10.1021/jacs.8b07113

Terms of use:

Open Access

Anyone can freely access the full text of works made available as "Open Access". Works made available under a Creative Commons license can be used according to the terms and conditions of said license. Use of all other works requires consent of the right holder (author or publisher) if not exempted from copyright protection by the applicable law.

(Article begins on next page)

Autoluminescent Metal Organic Frameworks: Self-Photoemission of a Highly Stable Thorium MOF

Jacopo Andreo^{†*}, Emanuele Priola[†], Gabriele Alberto[†], Paola Benzi^{†‡}, Domenica Marabello^{†‡}, Davide M. Proserpio^{‡c}, Carlo Lamberti^{‡#§} and Eliano Diana^{†‡*}

[†] Department of Chemistry, University of Turin, Via Pietro Giuria 7, 10125, Turin, Italy.

[‡] CrISDi, Interdepartmental Center for Crystallography, Via Pietro Giuria 7, 10125, Turin, Italy.

^{‡c} Dipartimento di Chimica, Università degli Studi di Milano, Via Golgi 19, 20133 Milano, Italy.

^c Samara Center for Theoretical Materials Science (SCTMS), Samara State Technical University, Molodogvardeyskaya St. 244, Samara 443100, Russia.

[#] Department of Physics, Interdepartmental NIS Centre, University of Turin, Via Pietro Giuria 1, 10125, Turin, Italy.

[§] IRC "Smart Materials", Southern Federal University, Zorge Street 5, Rostov-on-Don, Russia.

Keywords: AUTOLUMINESCENCE, RADIOLUMINESCENCE, THORIUM, MOF, NAPHTHALENDICARBOXYLATE, SCINTILLATION

ABSTRACT: A novel thorium (IV) MOF, Th(2,6-naphthalenedicarboxylate)₂, has been synthesized via solvothermal reaction of thorium nitrate and 2,6-naphthalenedicarboxylic acid. This compound shows a new structural arrangement with an interesting topology and an excellent thermal resistance, as the framework is stable in air up to 450 °C. Most notably this MOF, combining the radioactivity of its metal center and the scintillation property of the ligand, has been proven capable of spontaneous photon emission.

1. INTRODUCTION

Radioluminescence is one of the most fascinating properties related to radioactivity. All radioactive materials spontaneously emit photons through several physical phenomena. However, an extremely high radioactivity and sample quantity are required to make it perceivable, as the majority of these phenomena present low emission efficiency. The most interesting exception to this general rule is scintillation, a luminescence whose energy source is a direct ionizing particle or a high-energy photon. These interact with the scintillator (a phosphor with scintillating property) triggering multiple excitations and leading to a burst of light, whose intensity depends only on the particle nature and energy, and the scintillator efficiency.¹

In the past, self-induced radioluminescent systems based on scintillation have been produced by simply mixing a strong radioactive emitter with an inorganic scintillator, but to the best of our knowledge just one mono-phasic crystalline system has ever been synthesized (ThBr₄), whilst no metal-organic material with this feature has ever been reported. This article means to design, synthesize and characterize a Metal-Organic Framework (MOF) that emits photons upon the interaction between the ionizing particles produced by the metal centers and the scintillating organic linkers, i.e. autoluminescence.^{2,3}

In the past fifteen years, MOFs⁴ have been drawing increasing attention due to a wide range of applications that include gas storage,⁵ adsorption,⁶ molecular sieves,⁷ catalysis⁸

and photocatalysis,⁹ leading to the synthesis of many new compounds. More recently, a promising development has been observed in the field of luminescent MOFs, aimed at the production of sensors and diodes.¹⁰ Despite all the scientific and technological interest in this class of materials, until now only few studies have involved radioactive metals, none of which takes into account their radioactivity neither in their characterization nor in their potential applications.

As shown by Allendorf and co-workers, MOFs may have scintillating properties, and may be advantageous over classical organic scintillators, owing to their better resistance to the damage caused by radioactive particles. An autoluminescent MOF, besides having the same scintillating properties, would be a ratiometric sensor, as its continuous emission of particles with a specific energy provides a constant internal reference.¹¹

Autoluminescent MOFs featuring a porous structure may find applications as sensors, with guest species tuning the autoluminescence. Two mechanisms may be involved, i) a decrease in luminescence, owing to the ionizing particle energy loss due to interactions with the guest; ii) an intermolecular interaction induced tuning of the luminescent properties of the organic linkers.

To achieve a self-induced radioluminescent system, we designed a synthesis based on a new simple idea. The two MOF components may also be the two components of an autoluminescent system: a radioactive element and a scintillator.

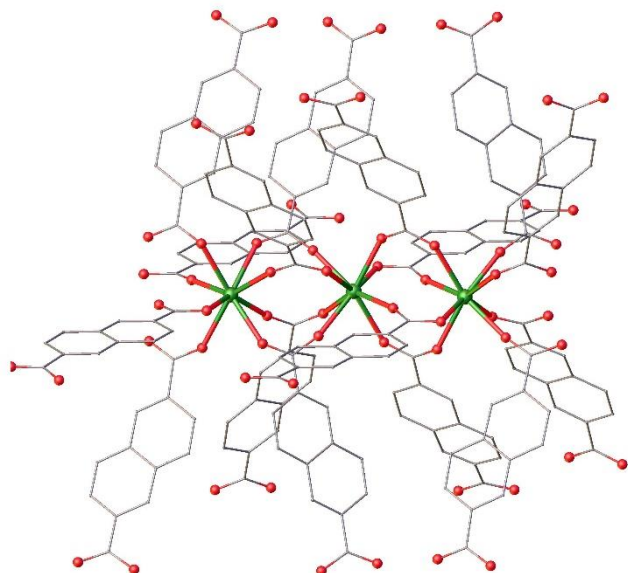


Figure 1. Rows of connected thorium atoms along the [101] direction in $\text{Th}(\text{NDC})_2$ MOF. Hydrogens are omitted for clarity. Th (green), O (red), C (gray).

Autoluminescence results from the interaction of the radio-emitted ionizing particles with the scintillator. The mechanism is the following: i) the scintillator is ionized by the ionizing particle; ii) core-hole recombination takes place, leaving the system in an electronic excited state; iii) the system decays to the ground state through visible light emission.

An appropriate metal center should not only be radioactive, but also avoid interference with the luminescence of the linker. To achieve this we have chosen thorium, as: i) it emits low penetration alpha particles that release most, if not all, of their energy inside the MOF lattice, thus maximizing photoemission; ii) the Th^{4+} cation is a closed-shell system, which prevents charge transfer transitions and, therefore, quenching phenomena that may reduce luminescence; iii) its extremely low radioactivity make thorium easier to handle than other radioactive metals. Finally, its behavior as MOF component is well known, yielding structures that are stable to air and water exposure. As metal center, Th^{4+} shows three different behaviours, depending on its ligands. If bound to carboxylate ligands only, thorium shows a strong preference for the square antiprism coordination geometry, with the ions disposed in a chain-like structure and the carboxylates bridging two vertices of adjacent cations. If O^{2-} anions are also present in the structure, the metal will rather arrange in octahedral clusters of six thorium cations, bridged by eight oxygen anions, that are fairly common also in presence of light halogen anions or complexing solvents (N,N-dimethylformamide or dimethyl sulfoxide). With any other type of ligand, thorium prefers an isolated metal centre geometry, coordinated by 8 or 9 ligands.^{12,13}

2,6-naphthalenedicarboxylate (NDC) was chosen as ligand due to its proven efficiency as scintillator. Its rigid aromatic architecture encourages luminescence emission and a rigid 3D structure, avoiding excessive flexibility and conformational freedom, which may quench or unpredictably modify the fluorescence and scintillating properties of the MOF.¹¹

2. EXPERIMENTAL SECTION

Caution! Thorium nitrate ($\text{Th}(\text{NO}_3)_4 \cdot 5\text{H}_2\text{O}$) is a radioactive reactant, suitable precautions must be followed for its handling. $\text{Th}(\text{NDC})_2$ (thorium bis-2,6-naphthalenedicarboxylate) was prepared heating a solution of 0.1 mmol of $\text{Th}(\text{NO}_3)_4 \cdot 5\text{H}_2\text{O}$ (57.0 mg) and 0.3 mmol of 2,6-naphthalenedicarboxylic acid (2,6-NDCA) (64.8 mg) in 5 ml of N,N-dimethylformamide (DMF) in a 50ml Parr autoclave at 383 K for 7 days. The resulting pale yellow crystalline powder was then centrifuged, washed three times in DMF and dried at room temperature in air. Yield: 61.5 mg, 93.1%. This compound was also synthesized by heating a mixture of 0.1 mmol of $\text{Th}(\text{NO}_3)_4 \cdot 5\text{H}_2\text{O}$ (57.0 mg), 0.3 mmol of ligand (64.8 mg) and 5 ml of H_2O in a 50ml Parr autoclave at 383 K for 7 days. Yield: 59.9 mg, 90.7%. The resulting yellowish powder was then centrifuged, washed three times in DMF and dried at room temperature in air. The second method afforded suitable crystals for X-ray single crystal diffraction. The purity of the product has been checked with elemental analysis: calculated C 43.65%, H 1.83%, O 19.38%; found C 43.2%, H 1.9%, O 19.5%.

3. RESULTS AND DISCUSSION

$\text{Th}(\text{NDC})_2$ crystallizes in the monoclinic space group $\text{C2}/c$ in form of small prismatic crystals of pale yellow color. The structure is built by rows of octa-coordinated thorium atoms with distorted square antiprism geometry that run along the [101] direction (Figure 1). Thorium ions are bridged by four carboxylate groups with variable Th-O distances in the range $2.310 \div 2.508 \text{ \AA}$, resulting in alternating $-\text{Th}(\text{COO})_4\text{Th}-$ bridges with Th...Th separations of 4.36 and 4.76 \AA (Figure 2a). NDC molecules cross-link the metal rows, yielding a three-dimensional MOF. Triangular void channels are highlighted in the (101) view of the crystal (Figure 2b). The underlying net of the rod-MOF

$\text{Th}(\text{NDC})_2$ is derived by taking the two midpoints between the Th atoms and connecting them to the carbon atoms of the carboxylate bridges as shown in Figure 2a, resulting in

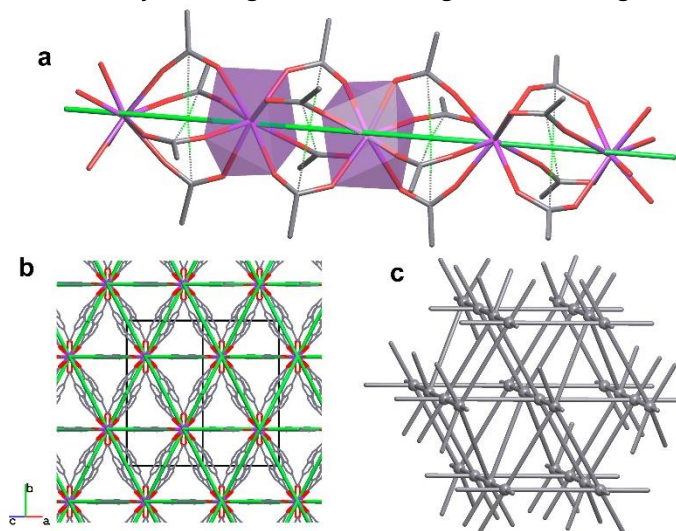


Figure 2. View of the crystal structure in the (101) plane of $\text{Th}(\text{NDC})_2$ MOF. Hydrogens are omitted for clarity.

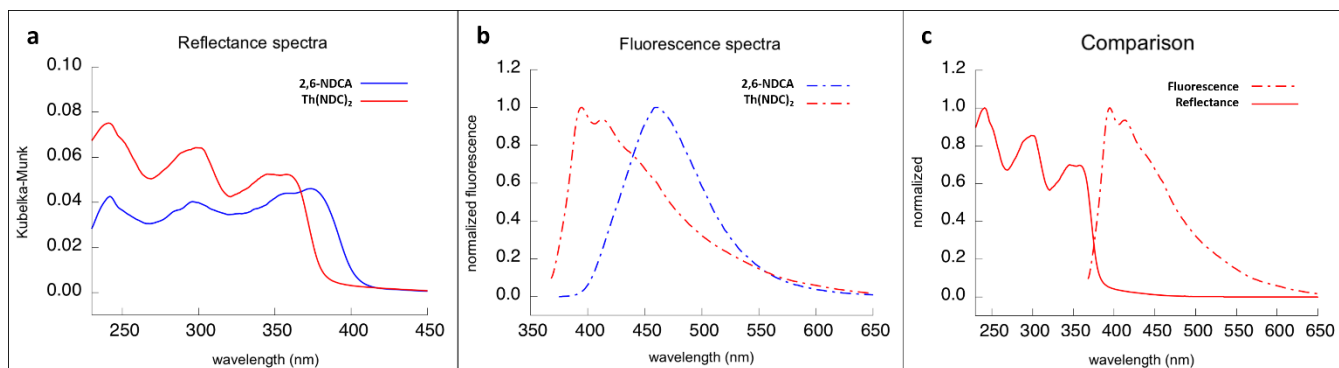


Figure 3: a- comparison between the reflectance spectra of the MOF and of the ligand. b- comparison between the fluorescence spectra of the MOF and the ligand. The wavelength of excitation is 345nm. c- comparison between reflectance and fluorescence of ThNDC₂.

a new binodal 6-c net with point symbol $(3.4^2.5^7.6^5)(3^2.4^2.5^5.6^4.7^2)$ (Figure 2c).¹⁴ Furthermore, the view down (101) shows that the parallel rods are efficiently packed as a hexagonal lattice (Figure 2b).¹⁵ More details on the topology are available in the Supplementary Information (Figures S3-S8).

The single-crystal-simulated powder X-ray diffraction pattern is comparable with the experimental powder pattern, confirming the quality of the results (Figure S9). The same Figure shows a pattern collected 1 year later: the excellent agreement between the two proves that crystallinity is not damaged neither by alpha-emission nor by air exposure in the medium-long time range.

Vibrational spectroscopies (Figures S10, S11) provide a powerful tool for distinguishing between different compounds in MOF analysis. IR bands at 1655 cm⁻¹ and 451 cm⁻¹, assigned to the carboxylate group and to the metal-carboxylate bond respectively, provide informations on the success of the synthesis (Table S2 and Figure S10 and S11).¹⁶

ThNDC₂ has an excellent thermal stability: TGA analysis demonstrates that it is stable in air up to 450 °C, while the velocity of degradation has a maximum at 515 °C. The compound shows a single step loss of 60% of weight due to the complete degradation of the organic ligands (Figure S12), the remaining 40% corresponding to thorium oxide.

Krypton absorption, performed at 77 °K, shows no diffusion inside the MOF pores, with a BET of 0.4135 m²/g (Figure S13). This is due to the tilt of the NDCs on the (11-1) and (1-1-1) planes. These ligands, occluding the pores, prevent any gas absorption, despite the 22% of void that PLATOON calculations predict.

Figure 3a shows the diffuse reflectance spectra of the ligand and of Th(NDC)₂. Both samples were diluted 1:20 in silica to avoid saturation in the collection of the diffuse reflectance. It is possible to observe how the MOF scaffold affects ligand absorption, resulting in a small blue-shift of the two peaks at higher wavelength. Nevertheless, the shape of the absorption spectrum is roughly the same both for Th(NDC)₂ and the ligand, indicating that the transitions are only weakly perturbed by the insertion in the MOF framework. The three transitions have been assigned, by means of TD-

DFT (time-dependent density functional theory) calculations, as π to π^* ; specifically: HOMO-1 \rightarrow LUMO+1, HOMO-1

\rightarrow LUMO, the HOMO \rightarrow LUMO+1 and HOMO \rightarrow LUMO- for the components at 240, 300, 345 and 374 nm respectively.

Similar considerations may be drawn about the fluorescence spectra (Figure 3b). Again, the spectrum of the MOF is blue-shifted, with a small modification of its shape exhibiting better resolved bands. These observations are attributed to insertion in the rigid scaffold of the MOF,¹⁷ as the confinement of the ligand results in its impossibility to decay in certain vibronic states. This implies that the remaining transitions became more distant in energy, thus resulting in a better resolved spectrum.

Figure 3c shows the normalized absorbance and fluorescence spectra of the MOF. The two spectra present only a small overlap, which results in a very small contribution of self-absorption to the fluorescence quenching. Moreover, if we consider that a scintillation spectrum is red-shifted compared to the fluorescence one, this contribution becomes negligible in terms of scintillation quenching, and thus in terms of autoluminescence^{1,11}.

Absolute quantum yield was also measured on solid samples by coupling Quanta ϕ to a Horiba Jobin Yvon Fluorolog 3 equipped with a 450-W Xenon lamp and a R928 photomultiplier. In the case of the MOF a value of 39.84% (\pm 3%) was calculated, whereas a photoemission efficiency of 34.5(\pm 3%) was obtained for the organic ligand in the same experimental conditions. These data are in good agreement with those obtained by steady state fluorescence measurements, indicating an increase in the probability of the radiative decay process with respect to non-radiative ones due to the loss of molecular degrees of freedom experienced by the ligand constrained in the MOF scaffold.

Fluorescence lifetimes were measured using a time-correlated single photon counting (TCSPC) technique (Horiba Jobin Yvon) with excitation source NanoLed at 297 nm (Horiba) or at 370 nm (Horiba) and impulse repetition rate of 1 MHz at 90 degrees to a TBX-4 detector. The detector was set to the maximum of emission for the compound in exam, with a 5 nm band-pass. The instrument was set in the Reverse TAC mode, where the first detected photon represented the start signal by the time-to-amplitude converter

(TAC), and the excitation pulse triggered the stop signal. DAS6 decay analysis software was used for lifetime calculation. Both the ligand and the MOF show a decay composed by three different life-times (NDC: τ_1 3.56ns, 10%; τ_2 11.23ns, 49%; τ_3 23.13ns, 41%; χ^2 1.07. Th(NDC)₂: τ_1 0.63ns, 83%; τ_2 2.84ns, 9%; τ_3 14.09ns, 8%; χ^2 1.16). These data apparently appear in contrast with the quantum yields, as the ligand show much longer lifetimes. This discrepancy, however, is easily explained by the crystalline habit of the two materials: the NDC's is characterized by strong π interactions, that lead to the formation of excitons that prolong the lifetimes while quenching the fluorescence. On the contrary the MOF topology do not allow the formation of π staking among ligands, thus shortening the life times and removing the quench associated with this phenomenon.

With the aim of evaluating the self-induced radioluminescence, we employed a Packard Tri-Carb 2200 CA liquid scintillator. This instrument uses two photomultiplier tubes connected to a coincidence circuit to detect the light pulses resulting from the scintillation response of a scintillator to an ionizing particle. This results in a high sensitivity, because this set up minimizes false signals from the photomultiplier tubes arising from the dark current. Since the instrument normally works on liquid solutions, we modified the standard procedure by placing a capillary tube with a diameter of 0.4 mm, bearing a known quantity of the sample, in the center of the vial employed by the instrument (Figure S14).

Initially, we determined the background signal of the instrument, using a tube filled with a radio-inactive compound: recrystallized NaF was found suitable for this, as both its elements present a unique stable isotope with a natural abundance of 100%. Using this set up, the instrumental noise was determined at 31 counts per minute (c.p.m.), in-

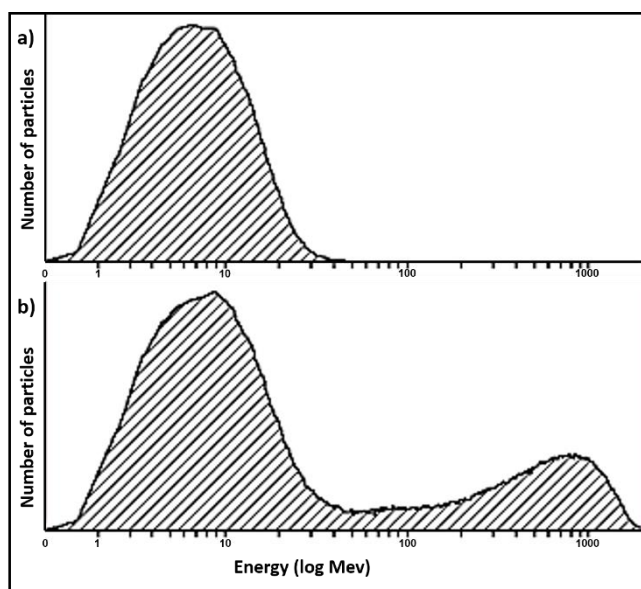


Figure 4: a) Energy profile of the particle detection of the MOF. b) Energy profile of the particle detection of the MOF submerged in the liquid scintillator.

dependently of the mass sample, and this value was subtracted from any raw data collected with this instrumental protocol.

The 2,6-naphthalendicarboxylic acid performed similarly, with results comparable to the base value. Th(NO₃)₄·5H₂O yielded 10.9 count per minute per milligram (0.42 mg of thorium). This value corresponds roughly to the 10% of the particles emitted by the thorium. Th(NDC)₂ has a count per minute per milligram (0.35 mg of thorium) ratio of 173.0, meaning that roughly 200% of the ionizing particles that are emitted produce enough photons to be detected, resulting in a twenty-fold enhancement of the autoluminescence. This value exceeds 100% because the scintillation counter usually works with aqueous solutions of organic scintillators, which present a much faster recombination of the ionized states induced by ionizing particles, compared to a solid system. This implies that the flash of photons emitted by the MOF, when it interacts with an ionizing particle, is sensibly longer than the one produced by the liquid scintillator. For this reason, the instrument recognizes every burst of the MOF as two separate events, doubling the count. The measurements on a mixture of Th(NO₃)₄·5H₂O and NDC in a ratio of 1:2, grinded separately and then mixed together to avoid a solid-state reaction, resulted in a count equivalent to the 168% of the particles emitted, meaning that only the 84% of the decay events of the thorium may be revealed by the simple mixture of the two MOF components. This prove that a mixing at the molecular level and a crystalline structure strongly improve the autoluminescent properties of the system. This is even more interesting when combined with the resilience of the MOF to the damage inflicted by the particles emitted by the thorium centers: as the MOF crystallinity is unaffected after one year, similarly its autoluminescence count do not vary.

To further prove that the instrument response is triggered only by the MOF's autoluminescence two additional experiments were designed and performed. The first was carried on submerging the capillary in a liquid scintillator (Ultima Gold AB, from Perkin Elmer, SP8S3), thus avoiding the presence of air in the vial, which could interact with the alpha particles that could leave the capillary, and the beta particles originated from thorium's family decay (that are very few, because the members of the decay chain did not have enough time to reach the equilibrium). The photon counter, as expected, improved, but the profile of the particle detection of this system shows two distinct peaks: one analogous to that of the MOF and one relative to the liquid scintillator (Figure 4). The second experiment was aimed at proving that the instrumental signal was not generated by gamma rays. To do this, we simply wrapped the capillary in black paper, as it is able to block most of the visible and U-V light but is transparent to photons with higher energies. With this set-up, the particle counter dropped to 16.8 per minute per milligram, proving that the measurements reported in Figure 4 are not influenced by gamma-rays.

4. CONCLUSIONS

To summarize, this work presents a thorium MOF, with a novel structure and a complex new topology. Remarkably (see SI), the MOF is stable up to 450 °C in air and its frame-

work is not affected by aging (in one-year scale). Furthermore, we proved how this MOF, combining the alpha-particle emission typical of thorium with the scintillating properties of the 2,6-naphthalenedicarboxylate, spontaneously emits photons, resulting in the first autoluminescent MOF. Finally, this is the first reported case of a metalloorganic framework with a property directly connected with the radioactivity of its metal centre. These two factors prove that rational design leads to new and exotic properties in MOFs. Properties that may be linked to uncommon or unfashionable sources, in this case radioactivity. What is certain is that we are only beginning to explore an exciting new area of chemistry and functional materials.

ASSOCIATED CONTENT

X-ray Structure determination and structural data, X-ray powder patterns, computational details, IR and Raman spectra, thermogravimetric curve and CIF files. This material is available free of charge via Internet at <http://pubs.acs.org>.

AUTHOR INFORMATION

Corresponding Author

Prof. Eliano Diana
Email: eliano.diana@unito.it

Jacopo Andreo, MSc
Email: jacopo.andreo@studenti.unipr.it

Author Contributions

The manuscript was written through contributions of all authors. / All authors have given approval to the final version of the manuscript. / ‡These authors contributed equally. (match statement to author names with a symbol)

ACKNOWLEDGMENT

We thank professor Alessandro Lo Giudice and doctor Francesca Peccati for useful suggestions and discussions. C.L. acknowledges the mega-grant of Ministry of Education and Science of the Russian Federation (14.Y26.31.0001).

ABBREVIATIONS

MOF, Metal Organic Framework;
NDC, 2,6-naphthalenedicarboxylate;
2,6-NDCA, 2,6-naphthalenedicarboxylic acid;
DMF, N,N-dimethylformamide;
Th(NDC)₂, thorium bis-2,6-naphthalenedicarboxylate;
TD-DFT, time-dependent density functional theory;
TCSPC, time-correlated single photon counting;
TAC, time-to-amplitude converter;
c.p.m., counts per minute.

REFERENCES

- (1) a. Birks J. B. *The theory and practice of scintillation counting*. Pergamon Press, **1964**. b. Blasse G., *Chem. Mat.* **1994**, *6*, 1465-1475. c. Milbrath B. D.; Peurrung A. J.; Bliss M.; Weber W. J. *J. Mater. Res.* **2008**, *23*, 2561-2581. d. Nikl M.; Yoshikawa A. *Adv. Opt. Mater.* **2015**, *3*, 463-481.
- (2) a. Carlier R.; Genet M. *Comp. Rend. C.* **1975**, *281*, 671. b. Genet M.; Hussonnois M.; Krupa J. C.; Carlier R.; Guillaumont R. *J. Luminescence.* **1976**, *12*, 953.
- (3) Carlier R.; Krupa J.C.; Hussonnois M.; Genet M.; Guillaumont R. *Nucl. Instr. Meth.* **1977**, *143*, 613-615.
- (4) a. Yaghi, O. M.; O'Keeffe, M.; Ockwig, N. W.; Chae, H. K.; Eddaoudi, M.; Kim, J. *Nature*, **2003**, *423*, 705-714. b. Furukawa, H.; Cordova, K. E.; O'Keeffe, M.; Yaghi, O. M. *Science*, **2013**, *341*, 974. c. Batten S. R.; Champness N. R.; Chen X.-M.; Garcia-Martinez J.; Kitagawa S.; Öhrström L.; O'Keeffe M.; Paik Suh M.; Reedijk J. *Cryst. Eng. Comm.*, **2012**, *14*, 3001-3004
- (5) a. Morris, R. E.; Wheatley, P. S. *Angew. Chem.-Int. Edit.* **2008**, *47* (27), 4966-4981. b. Ma, S. Q.; Zhou, H. C. *Chem. Commun.* **2010**, *46* (1), 44-53. c. Dinca, M.; Yu, A. F.; Long, J. R. *J. Am. Chem. Soc.* **2006**, *128* (27), 8904-8913. d. Millward, A. R.; Yaghi, O. M. *J. Am. Chem. Soc.* **2005**, *127* (51), 17998-17999. e. Eddaoudi, M.; Kim, J.; Rosi, N.; Vodak, D.; Wachter, J.; O'Keeffe, M.; Yaghi, O. M. *Science*, **2002**, *295*, 469-472
- (6) a. Li, J. R.; Kuppler, R. J.; Zhou, H. C. *Chem. Soc. Rev.* **2009**, *38* (5), 1477-1504. b. Sumida, K.; Rogow, D. L.; Mason, J. A.; McDonald, T. M.; Bloch, E. D.; Herm, Z. R.; Bae, T. H.; Long, J. R. *Chem. Rev.* **2012**, *112* (2), 724-781.
- (7) Li J.-R.; Sculley J.; Zhou H.-C. *Chem. Rev.* **2012**, *112*, 869-932.
- (8) a. Lee, J.; Farha, O. K.; Roberts, J.; Scheidt, K. A.; Nguyen, S. T.; Hupp, J. T. *Chem. Soc. Rev.* **2009**, *38* (5), 1450-1459. b. Corma, A.; Garcia, H.; Xamena, F. *Chem. Rev.* **2010**, *110* (8), 4606-4655. c. Vermeulen N. A.; Karagiari O.; Sarjeant A. A.; Stern C. L.; Hupp J. T.; Farha O. K.; Stoddart J. F. *J. Am. Chem. Soc.* **2013**, *135*, 14916-14919. d. Butova V. V.; Soldatov M. A.; Guda A. A.; Lomachenko K. A.; Lamberti C. *Russ. Chem. Rev.* **2016**, *85*, 280-307. e. S. M. J. Rogge, A. Bavykina, J. Hajek, H. Garcia, A. I. Olivos-Suarez, A. Sepúlveda-Escribano, A. Vimont, G. Clet, P. Bazin, F. Kapteijn, M. Daturi, E. V. Ramos-Fernandez, F. X. Llabrés i Xamena, V. Van Speybroeck and J. Gascon *Chem. Soc. Rev.* **2017**, *46*, 3134-3184.
- (9) Zhang, T.; Lin, W. *Chem. Soc. Rev.* **2014**, *43*, 5982-5993
- (10) a. Dou Z.; Yu J.; Cui Y.; Yang Y.; Wang Z.; Yang D.; Qian G. *J. Am. Chem. Soc.* **2014**, *136*, 5527-5530. b. Bauer C. A.; Timofeeva T. V.; Settersten T. B.; Patterson B.D.; Liu B. A.; Simmons V. H.; Allendorf M. D. *J. Am. Chem. Soc.* **2007**, *129*, 7136-7144. c. Heine J.; Muller-Buschbaum K. *Chem. Soc. Rev.* **2013**, *42*, 9232-9242. d. Kreno L. E.; Leong K.; Farha O. K.; Allendorf M.; Van Duyne R. P.; Hupp J. T. *Chem. Rev.* **2012**, *112*, 1105-1125.
- (11) a. Cui Y.; Yue Y.; Qian G.; Chen B. *Chem. Rev.* **2012**, *112*, 1126-1162. b. Doty F. P.; Bauer C. A.; Skulan A. J.; Grant P. G.; Allendorf M. D. *Adv. Mater.* **2009**, *21*, 95-101. c. Perry J. J. IV; Feng P. L.; Meek S. T.; Leong K.; Doty F. P.; Allendorf M. D. *J. Mater. Chem.* **2012**, *22*, 10235-10248. d. Mathis S. R. II; Golafale S. T.; Bacsa J.; Steiner A.; Ingram C. W.; Doty F. P.; Audene E.; Hattare K. *Dalton Trans.* **2017**, *46*, 491-500. e. Mathis S. R. II; Golafale S. T.; Solntsev K. M.; Ingram C. W. *Crystals*, **2018**, *8*, 53.
- (12) Falaise C.; Charles J. S.; Volkringer C.; Loiseau T. *Inorg. Chem.* **2015**, *54*, 2235-2242.
- (13) a. Falaise C.; Volkringer C.; Loiseau T. *Inorg. Chem. Comm.* **2014**, *39*, 26-30. b. Ok K. M.; Sung J.; Hu G.; Jacobs R. M. J.; O'Hare D. *J. Am. Chem. Soc.* **2008**, *130*, 3762-3763. c. Kim J.-Y.; Norquist A.; O'Hare D. *J. Am. Chem. Soc.* **2003**, *2*, 12688-12689. d. Ok K. M.; O'Hare D. *Dalton Trans.* **2008**, *41*, 5560. e. Ramaswamy P.; Prabhu R.; Natarajan S. *Inorg. Chem.* **2010**, *49*, 7927-7934. f. Thuéry P. *Eur. J. Inorg. Chem.* **2014**, *1*, 58-68. g. Thuéry P. *Inorg. Chem.* **2011**, *50*, 1898-1904. h. Li Y.; Yang Z.; Wang Y.; Bai Z.; Zheng T.; Dai X.; Liu S.; Gui D.; Liu W.; Chen M.; Chen L.; Diwu J.; Zhu L.; Zhou R.; Chai Z.; Albrecht-Schmitt T. E.; Wang S. *Nat. Commun.* **2017**, *8*, 1354.
- (14) a. Alexandrov, E. V.; Blatov, V. A.; Proserpio, D. M. *CrystEngComm* **2011**, *13*, 3947-3958. b. Schoedel, A.; Li, M.; Li, D.; O'Keeffe, M.; Yaghi, O. M. *Chem. Rev.* **2016**, *116*, 12466-12535.
- (15) a. O'Keeffe M.; Anderson S. *Acta Cryst.* **1977**, *33*, 914-923. b. Rosi, N. L.; Kim, J.; Eddaoudi, M.; Chen, B.; Yaghi, O. M. *J. Am. Chem. Soc.* **2005**, *127*, 1504-1518.
- (16) Bonino F.; Lamberti C.; Bordiga S. "IR and Raman Spectroscopies Probing MOFs Structure, Defectivity, and Reactivity", in *The*

Insert Table of Contents artwork here

